Environment International, Vol. 17, pp. 559-574, 1991
Printed in the U.S.A. All rights reserved.

0160-4120/91 $3.00 + .00

A PROCEDURE TO ESTIMATE WORST-CASE AIR QUALITY IN COMPLEX TERRAIN*

Roger A. Pielke and Roger A. Stocker
Department of Atmospheric Science, Colorado State University, Fort Collins, CO 80523

Raymond W. Arritt
Department of Physics and Astronomy, University of Kansas, Lawrence, KS 66045

Richard T. McNider
Department of Mathematics and Statistics, University of Alabama at Huntsville, Huntsville, AL 35899

EI 9006-145M (Received 6 June 1990; accepted 28 February 1991)

Using a straightforward synoptic climatological analysis scheme, it is shown that the potential for an area to experience air quality degradation due to local sources is highest under polar subtropical highs. With respect to polar highs, the problem is most severe when the sun angle is low and snow covers the ground, and the polar high persists for a long period of time. A simple algorithm is introduced which is designed to estimate worst-case impact in a trapping valley. The potential for the accumulation of air pollution in such valleys due to the persistence of a polar high in a region, is ignored in current regulatory air quality assessments. Trapping valleys and synoptic flow stagnation often occur in wilderness areas. Refined air quality assessments are shown to be possible using a mesoscale meteorological model and a pollution dispersion model. These tools permit quantitative assessments of pollution build-up from local sources as a result of the recirculation of the local air. This tool, along with the synoptic climatological classification scheme, also permits an evaluation of the fractional contribution of long range versus local sources in the air quality degradation in a region. Areas near the center of a polar or subtropical surface high pressure system, for instance, appear to be dominated by local sources, if they exist, whereas in the vicinity of extratropical cyclones, long-range transport is usually much more important.

INTRODUCTION

One of the reasons for formally establishing wilderness areas is to preserve regions in which the impact of man is minimal. This is the rationale for the goal to ban motorized vehicles, permanent structures, and roads in such areas. Unfortunately, however, man can impact these purportedly pristine areas in a direct fashion through the movement of air pollution. In United States National Park areas, Everhart (1983), concludes that air pollution is the single most important threat to the quality of the National Park system.

The purpose of this paper is two-fold:
(1) To identify those synoptic meteorological conditions in which the impact of air pollution would be most pronounced. As will be shown in the next section of this paper, the frequency with which specific synoptic conditions occur will be shown to vary across the United States and from season to season. This suggests that the potential for air quality degradation in wilderness areas will depend on where they are located, in addition to the magnitude of emissions from nearby pollution sources.
(2) Since existing observations in and adjacent to wilderness areas are invariably insufficient to adequately characterize the wind flow and turbulence within these areas, mesoscale meteorological models, as dis-

*Presented in the National Wilderness Research Conference: Issues, State-of-Knowledge, Future Directions.

cussed in Section *Mesoscale analyses* of this paper, represent an alternative tool for needed meteorological assessments. The atmospheric conditions are generated by the interaction of meteoro-logical circulations driven by differential gradients in the terrain surface with synoptic features in the overlying atmosphere.

The need to adequately characterize the meteorology in and near wilderness areas is paramount if accurate estimates of air pollution effects are to be achieved. As discussed in Section *Mesoscale analyses* of this paper, current regulatory tools used to assess worst case air quality impact in complex terrain, often very inaccurate and misleading, are ten to twenty years behind current technological capabilities.

AIR QUALITY CLIMATOLOGY

Classification of the general circulation

The general circulation of the earth can be schematically conceptualized into major regions, as illustrated in Fig. 1. The regions dominated by persistent subsidence are associated with deserts, while regions with average ascending motion generally have significant precipitation. These regions of average upward and downward motion move poleward in the summer, equatorward in the winter. While the influence of continents, mountains, and other geographic features alter the specific pattern, the general circulation framework illustrated in Fig. 1 is a useful backdrop with which to discuss air quality characteristics.

From Fig. 1, the general ability of air pollution to disperse can be interpreted. Not surprisingly, sinking air creates inversions and stabilizes the atmosphere, thereby inhibiting pollution dispersal while ascending air destabilizes the air. Precipitation cleanses the troposphere through scavenging (e.g., acid rain) in both stratiform and convective precipitation and by ejecting pollutants into the stratosphere by deep convective storms (with a possible climatic effect, Lyons et al. 1986). In clear air, pollution mixing near the ground is enhanced when solar heating is strong, but dispersion is inhibited during the night as long- wave radiational cooling near the ground creates a low-level stable layer.

As suggested in the schematic represented by Fig. 1, pollutant dispersion potential is poorest in the polar regions during the winter. Not only is the region dominated by subsidence associated with the polar surface high pressure system, but there is little or no solar heating. Unless there are strong katabatic flows such as found, for example, in Antarctica, there will be poor dispersal of pollution. In contrast, pollutant dispersion is expected to be very efficient in the intertropical convergence zone where average ascent and strong solar heating occur during the day results in deep thunderstorm systems.

From this brief discussion, it appears that certain areas of the world will be more prone to pollution problems than others. We can estimate the regions

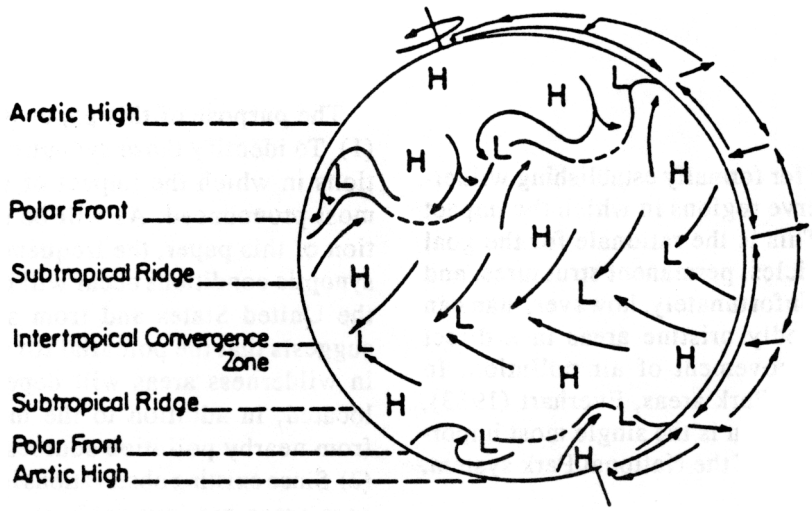

Fig. 1. Schematic of the general circulation of the earth in the northern hemisphere winter. There is average subsidence in the subtropical ridge and arctic high, and average ascent in the intertropical convergence zone and the polar front region (Pielke et al. 1987).

where these problems will be worse by considering their location relative to the large-scale circulation patterns of the atmosphere.

Synoptic classification

The United States, with the exception of Alaska, Hawaii, and a number of territories, is generally influenced by the southern portion of the polar high, the polar front, or the northern side of the subtropical ridge. Along the polar front, extratropical cyclones propagate which have different air quality dispersion characteristics in different parts of the cyclone.

Figure 2 presents an example of a weather map where cold and warm fronts on the polar front are indicated. Five major synoptic categories are defined

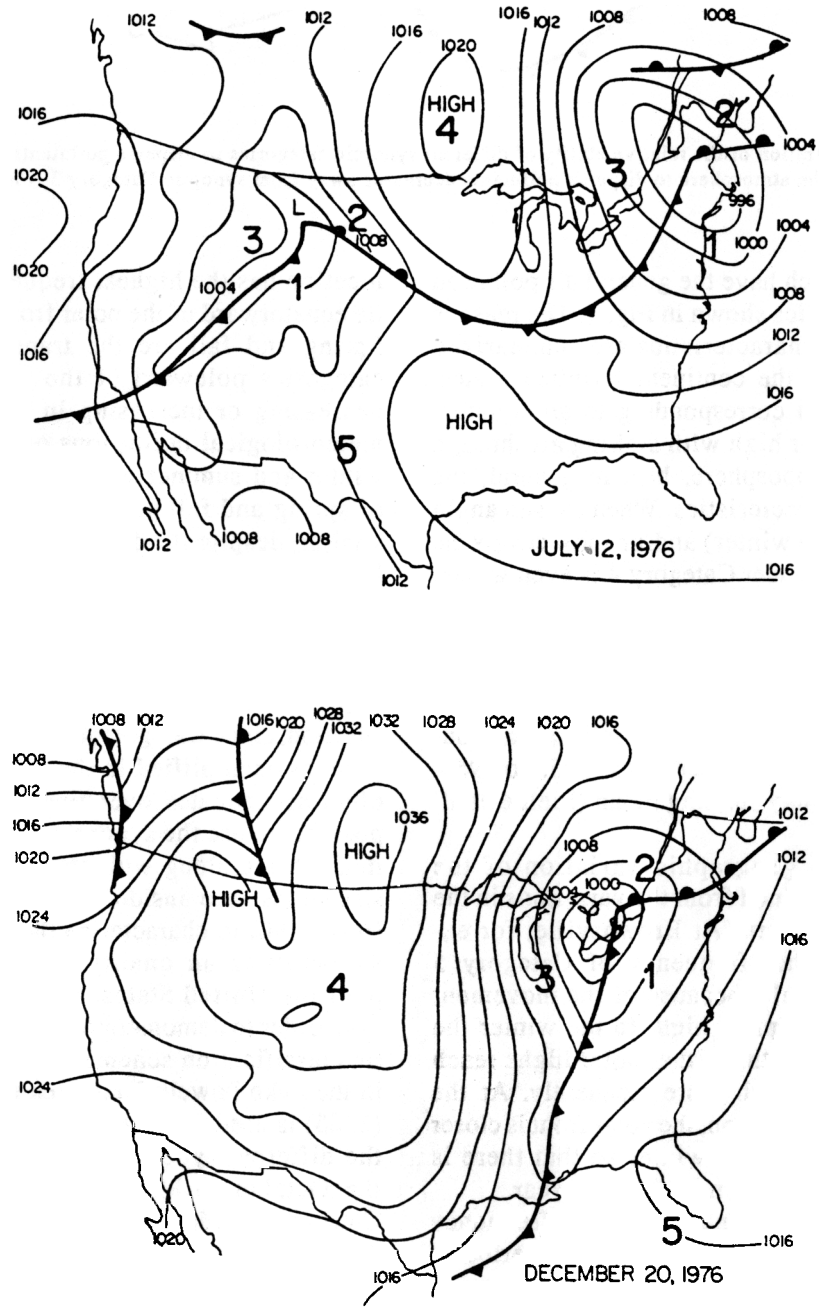

Fig. 2. Example of a surface analysis chart for 12 July 1976 and 20 December 1976 showing the application of the synoptic climatological model for the five synoptic classes listed in Table 1 (Pielke et al. 1987).

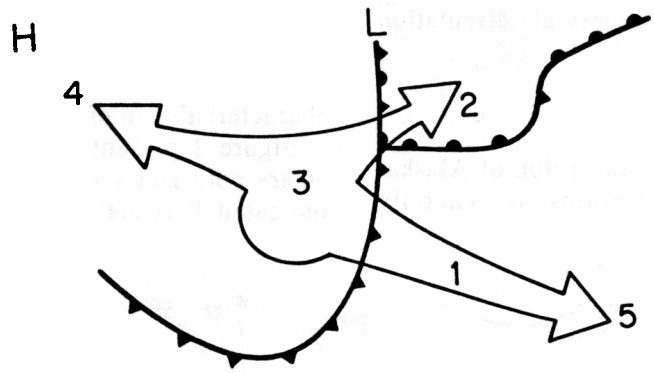

Fig. 3. Schematic illustration of the relative ability of different synoptic categories to disperse pollutants emitted near the ground. The ability of the atmosphere to disperse pollutants decreases away from synoptic Category 3 (Pielke et al. 1985).

in these examples which have the general air pollution dispersion characteristics shown in Fig. 3. The reasons for these dispersion characteristics are summarized in Tables 1 and 2. In the continental United States, Category 4, the region corresponding to an equatorward bulge in the polar high with sinking air through the lower and mid troposphere, has, in general, the poorest dispersion characteristics. When the sun angle is low (e.g., during the winter) and/or snow covers the ground, the dispersion under Category 4 is even worse.

The frequency of occurrence of the different synoptic categories varies during the year and from location to location. Figure 4 illustrates the variation of these categories for Brownsville, Texas; Mobile, Alabama; and Hampton, Virginia. This data was constructed from 10 years of weather maps (1955 to 1964, inclusive), with a 25-day running mean (Pielke et al. 1987).

The seasonal and geographic variation of the categories can be explained from the variations in the general circulation pattern. At Brownsville, for example, the much higher frequency of Category 5 during the summer results because of the movement northward of the subtropical high. In the winter the polar front is farther south, so that polar highs reach the Brownsville area much more frequently. At the more northerly site of Hampton, the polar front is closer during both the summer and winter so that there is less variability in the pattern during the year.

Seasons can also be defined using the frequency of the categories. Winter is defined as that period of the year when a site has the highest frequency of categories which occur poleward of the polar front (Categories 2, 3, and 4). Using this framework, summer corresponds to that time of the year when a location has the highest frequency of categories that lie equatorward of the polar front (Categories 1 and 5). Spring and fall are the transition times when the categories poleward of the front are, respectively, decreasing or increasing in frequency. Using these meteorological definitions of seasons, the length of winter and summer and the time of commencement of spring and fall at the different locations are very similar, despite the different latitudes of the cities in Fig. 4 (Fig. 5).

With these climatological definitions, the sensitivity of an area to air pollution degradation can be estimated. For the reasons listed in Table 2, Categories 2 and 4 are particularly prone to poor dispersion. In addition, since Category 4 often lasts a relatively long time, as exemplified in the next paragraph, pollution often accumulates over time within a region. It is possible to use the synoptic climatological classification scheme along with standard climatological classifications (see inside the cover of Trewartha and Horn 1980) to characterize the annual and geographic variability in air quality dispersion characteristics over the United States.

In order to demonstrate the usefulness of this synoptic classification scheme, the study of air stagnation in the Lake Powell, Utah area reported in Pielke et al. (1985) is used. In that investigation the occurrence of the different synoptic categories were evaluated for the October to May time periods of 1976 to 1981. Category 4, which, as has been discussed, is associated with poor air dispersion was evaluated for its persistence. During a persistent Category 4 event (in which no other categories sweep through to flush out any pollution), air quality is likely to deteriorate if local sources of emission exist.

Table 1. Synoptic classification scheme (Pielke 1982; modified from Lindsey 1980).

Category	Air Mass	Reason for Categorization*
1	*mT*	*In the warm sector of an extratropical cyclone.* In this region, the thickness and vorticity advection is weak with little curvature to the surface isobars. There is limited low level convergence with an upper level ridge tending to produce subsidence. Southerly low-level winds are typical.
2	*mt/cP, mT/cA, mP/cA*	*Ahead of the warm front in the region of cyclonic curvature to the surface isobars.* Warm air advecting upslope over the cold air stabilizes the thermal stratification, while positive vorticity advection and low-level frictional convergence add to the vertical lifting. Because of the warm advection, the geostrophic winds veer with height. Low-level winds are generally northeasterly through southeasterly.
3	*cP, cA*	*Behind the cold front in the region of cyclonic curvature to the surface isobars.* Positive vorticity advection and negative thermal advection dominate, with the resultant cooling causing strong boundary layer mixing. The resulting thermal stratification in the lower troposphere is neutral, or even slightly, superadiabatic. Gusty winds are usually associated with this sector of an extratropical cyclone. Because of the cold advection, the geostrophic winds back with height. Low-level winds are generally from the northwest through southwest.
4	*cP, cA*	*Under a polar high in a region of anticyclonic curvature to the surface isobars.* Negative vorticity, weak negative thermal advection and low-level frictional divergence usually occur, producing boundary layer subsidence. Because of relatively cool air aloft, the thermal stratification is only slightly stabilized during the day, despite the subsidence. At night, however, the relatively weak surface pressure gradient associated with this category causes very stable layers near the ground on clear nights due to long-wave radiational cooling. The low-level geostrophic winds are usually light to moderate varying slowly from northwesterly to southeasterly as the ridge progresses eastward past a fixed location.
5	*mT*	*In the vicinity of a subtropical ridge* where the vorticity and thickness advection, and the horizontal pressure gradient at all levels are weak. The large upper-level ridge, along with the anticyclonically curved low-level pressure field, produces weak but persistent subsidence. This sinking causes a stabilization of the atmosphere throughout the troposphere. Low-level winds over the eastern United States associated with these systems tend to blow from the southeast through southwest.

*This discussion applies to the northern hemisphere.

For the five-year study period, the average maximum duration of Category 4 was found to be 13.2 days with a maximum length of 18 days (Fig. 6). In another study which used the same classification scheme, a rectangular grid area with dimensions of 35° N - 37.5° N and 115° W - 120° W (this includes the Lake Powell area) was classified for the years 1980/1981 through 1986/1987. The first four years involved an analysis of eight months of data per year (October-May), and the last three years involved an analysis of only five months

Category Characteristics	Category 1	Category 2	Category 3	Category 4	Category 5
Category Class	*mT* In the warm sector of an extratropical cyclone.	*mT/cP, mt/cA, mP/cA* Ahead of the warm front in the region of cyclonic curvature to the surface.	*cP, cA* Behind the cold front in the region of cyclonic curvature to the surface isobars.	*cP, cA* Under a polar high in a region of anticyclonic curvature to the surface.	*mT* In the vicinity and west of a subtropical ridge.
Surface Winds	Brisk SW surface winds.	Light to moderate SE to ENE surface winds.	Strong NE to W surface winds.	Light and variable winds near the center of the high.	Light SE to SW winds.
Vertical Motion	Weakening synoptic descent as the cold front approaches.	Synoptic ascent due to warm advection and positive vorticity advection aloft.	Synoptic ascent due to positive vorticity advection aloft (in this region this ascent more than compensates for the descent due to cold advection).	Synoptic descent (due to warm advection and/or negative vorticity advection aloft).	Synoptic subsidence (descending branch of the Hadley cell). Becomes stronger as you approach the ridge axis.
Temperature Advection	Little temperature advection at the surface.	Warm advection above the frontal inversion.	Cold advection at the surface.	Weak temperature advection at the surface.	Weak temperature advection at the surface.
Inversion	Weak synoptic subsidence inversion caps planetary boundary layer.	Boundary layer capped by frontal inversion.	Deep planetary boundary layer.	Synoptic subsidence inversion and/or warm advection aloft create an inversion which caps the planetary boundary layer.	Synoptic subsidence inversion.
Diurnal Variation in Boundary Layer Stability	Moderate diurnal variability in the boundary layer stability.	Little diurnal variability in boundary layer stability because of cloud cover.	Little diurnal variability in the boundary layer stability because of strong winds and destabilizing of boundary layer by cold advection.	In the absence of snow cover because of clear skies and light winds. Large diurnal variability in boundary layer stability.	Moderate diurnal variability in boundary layer stability.
Diurnal Variation in Surface Layer Stability	Moderately unstable surface layer during the day. Moderately stable surface layer during the night.	Stably stratified surface layer day and night.	Near neutral surface layer day and night.	Weakly to moderately unstable surface layer during the day unless snow cover present or low sun angle in which case surface layer tends to be stably stratified. Very stable surface layer at night.	Moderately to strong unstable surface layer during the day. Moderate to strong stable surface layer during the night.
Humidity	Often humid in relative and absolute sense.	Often dry in absolute sense but humid in relative sense.	Dry in the absolute sense. Usually dry in the relative sense.	Dry in the absolute sense. Humid in the relative sense. At night, dry in the relative sense during the day except when ground is snow-covered and/or the low levels are cold.	Humid in the relative and absolute sense.
Cloud Cover	Clear to partly cloudy skies except near squall line.	Mostly cloudy to cloudy.	Clear to scattered or broken shallow convective clouds.	Clear except tendency for fog at night. Middle and/or high level clouds can be transported in by warm advection over the center and to the west of the polar high center.	Scattered fair weather cumulus in the day. Clear during the night except near the mesoscale systems listed below.

Table 2. Overview of meteorological aspects of the five synoptic categories illustrated in Fig. 1 (northern hemisphere) (modified from Pielke et al. 1985).

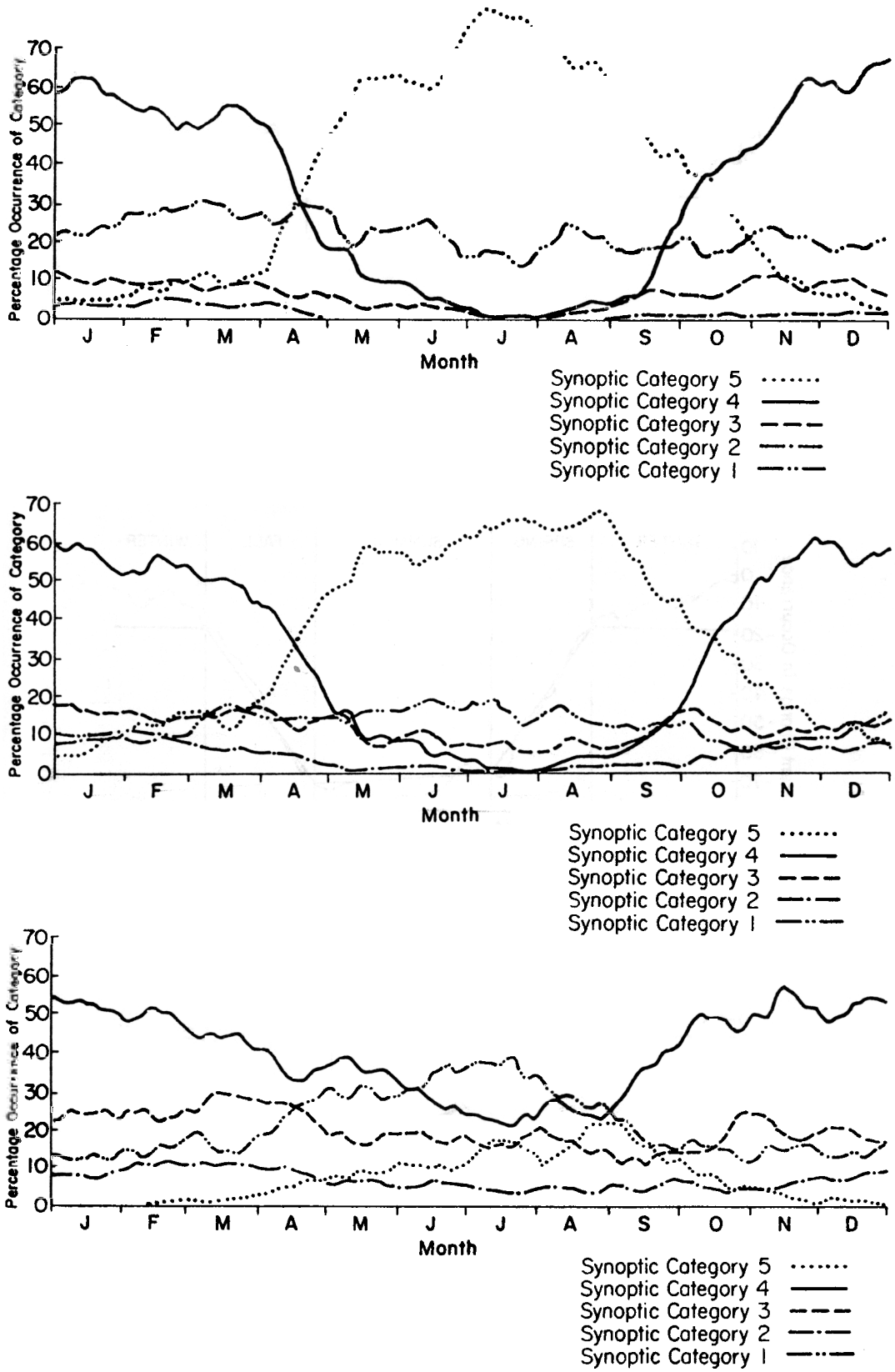

Fig. 4. Occurrence of synoptic categories (25-day average) for a) Brownsville, Texas, b) Mobile, Alabama, and c) Hampton, Virginia. The synoptic categories are defined in the legend (Pielke et al. 1987).

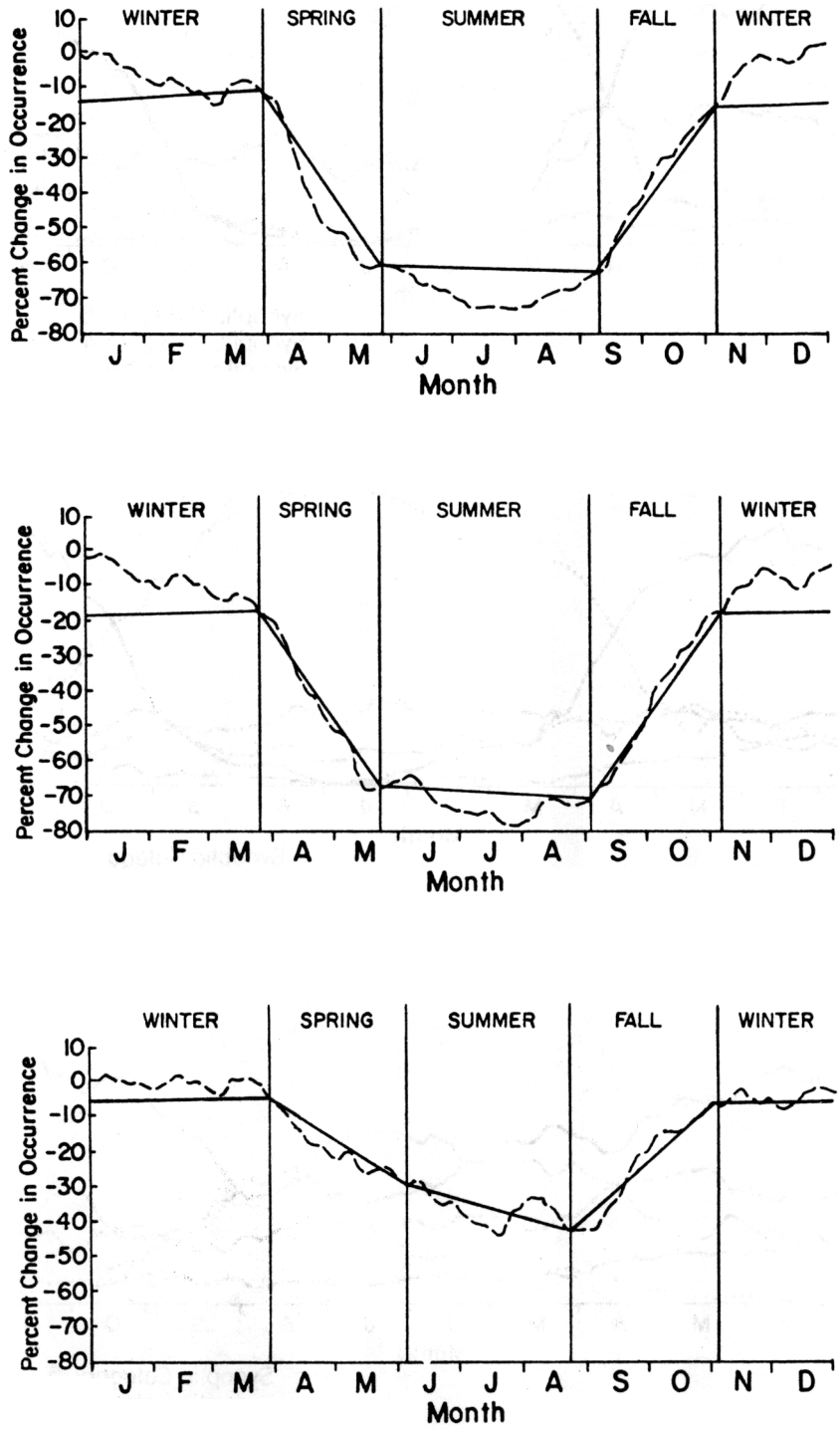

Fig. 5. Changes in frequency of occurrence of categories north of the polar front (dashed line) for a) Brownsville, Texas, b) Mobile, Alabama, and c) Hampton, Virginia. The solid line is the average over seasons which are meteorologically defined as given in Pielke et al. (1987).

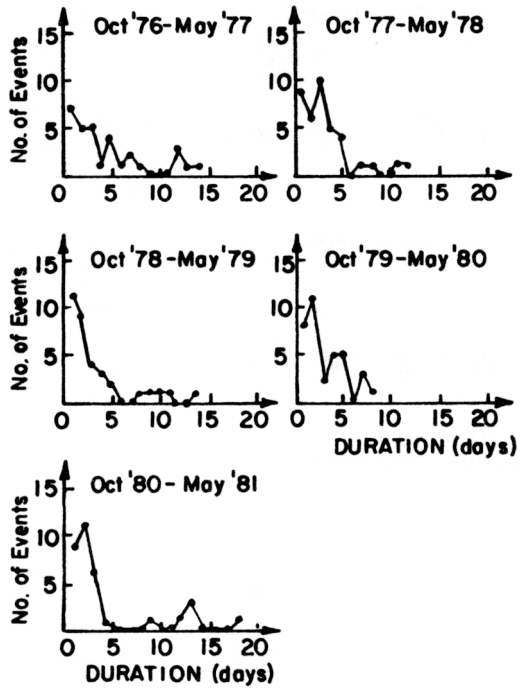

Fig. 6. Duration and number of events of Category 4 for the specified time periods (Pielke et al. 1985).

(November-March) . Since the synoptic classification scheme was applied over an area instead of a point, the possibility of multiple classifications (more than one synoptic category in an area on any given day) were considered in the persistence calculation. To this end, two types of persistence calculations were performed. In the first, if any subportion of the area contained a non-Category 4 region, the persistence event was terminated (these events are defined as conservative in Fig. 7). In the second analysis, if any portion of the area retained a Category 4 region, the persistence event continued (these events are defined as non-conservative events in Fig. 7).

Figure 7 shows the results of these analyses. The average length of a persistence event for the seven-year period (only persistence events longer than two days were considered) was 5.2 and 7.7 days for the conservative and non-conservative calculations, respectively. The longest persistence event was 23 and 43 days for the conservative and non-conservative calculations, respectively. Since the first four-year and last three-year analysis involved different time periods, the average persistence events were also calculated separately for each period. For the first four years, the average persistence event lasted 5.0 and 7.5 days for the conservative and non-conservative calculations, respectively. For the last three years, the average persistence was 5.7 and 9.5 days for the conservative and non-conservative calculations, respectively. This implies that most of the longer persistence events in this area occur between the months of November and March.

In a separate study for western Colorado using radiosonde soundings at Grand Junction, Colorado to characterize days with poor air quality dispersion, Hanson and McKee (1983) found similar results. In their study, during the December to January time period for 1959-1978, stagnation events lasted an average of 9 days with a maximum of 28 days in the 1976-1977 period. According to their study stagnation events 3 days or longer occur on the average nearly 7 times per year. Pielke et al. (1985) concluded that Category 4 conditions correspond, in general, to the situations of persistent stagnation as found by Hanson and McKee (1983).

From the above discussions and the related published studies, it is concluded that the climatological potential for poor (or good) air quality dispersion can be characterized with reference to the general circulation of the earth and to synoptic weather systems. In the next section, tools will be discussed which can assess worst-case air quality impacts in complex terrain.

MESOSCALE ANALYSES

Types of mesoscale systems

There are a wide range of atmospheric systems which are local in scale as discussed, for example, in Pielke (1984). These systems are referred to as being mesoscale. These include features which are associated with extra-tropical storms (e.g., squall-lines, embedded convection) as well as circulations that are forced by terrain irregularities (e.g., land and sea breezes, mountain-valley winds). The latter type of systems, frequently referred to as thermally-forced mesoscale systems, are most often associated with polar and subtropical surface high pressure systems (i.e., synoptic Categories 4 and 5, and the typical mesoscale systems are listed in Table 2). These thermally-forced mesoscale circulations are most well developed when the synoptic flow is weak or absent, such as often occurs in Category 4 and 5. Thermally-forced circulations develop because differential heating or cooling develops between adjacent locations. A circulation develops as the atmosphere responds to the horizontal temperature distribution.

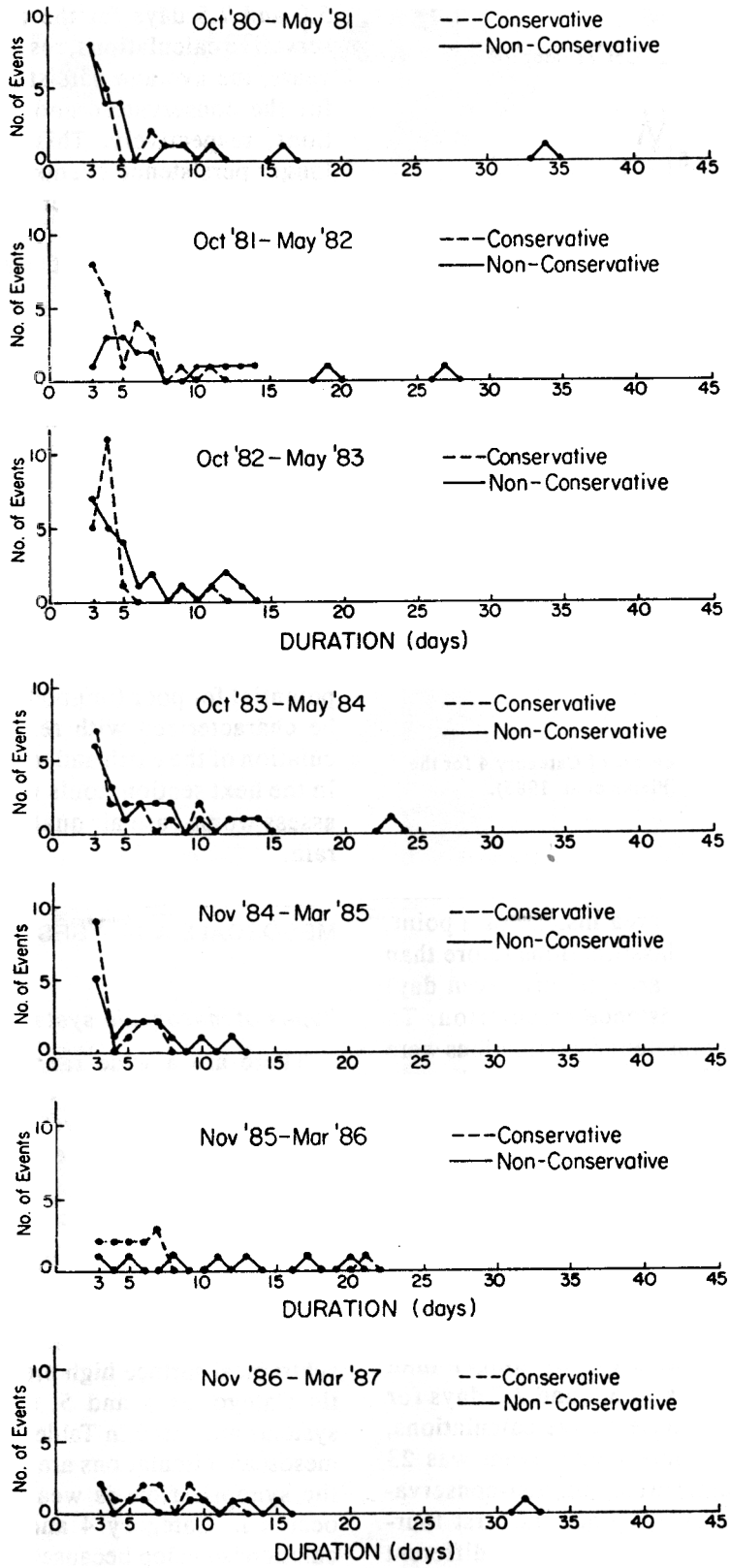

Fig. 7. Duration and number of events of Category 4 for an area representing Lake Powell, Utah. See text for definitions of conservative and non-conservative.

One type of thermally-forced system, the mountain-valley circulation, is particularly important in the air quality budget in irregular terrain. It is well-known that elevated topography acts as an elevated heat source during sunny days and as a heat sink on clear nights. The resultant wind flow is one in which air tends to move uphill during the day and downslope at night. This upslope/downslope flow tends to be confined to below the inversion height associated with the polar and subtropical high pressure systems. In rugged terrain, particularly in the winter and at times of low sun angles, this inversion is often confined below the heights of the higher terrain.

The potential for air quality degradation due to local sources of emission in irregular terrain exists during these meteorological situations. The accumulation of pollution in these mountain-valley circulations is expected to be greatest when the circulation is confined within a basin (as a result of the pooling of cold air), so that none of the effluent exits the region.

As discussed by McKee and O'Neal (1988), there are two types of mountain-valley systems. A trapping valley system is one in which the mountain-valley circulation is too shallow for air to be transported out of the basin, whereas a flushing valley system is one in which gaps and passes exist below the inversion height so that the pooled cold air can flow out. A flushing valley, therefore, has a mechanism to disperse locally generated pollution.

The trapping valley, therefore, represents the potential for the worst case of pollution due to local sources within that valley. Unfortunately, no existing regulatory air quality assessment tool is capable of estimating accumulations of air pollution within a trapping valley. Moreover, even flushing valleys can act as a trapping valley if the synoptic wind flow has nearly the same vertical temperature distribution and is equal and opposite in direction to the outflow of cold air from the valley.

Algorithm to estimate air quality degradation due to trapping

Despite the lack of attention by the regulatory agencies to trapping valleys, a very simple algorithm can be used to estimate potential or actual pollution impacts due to local sources within such a valley. This algorithm can be expressed

$$C = E\,t/(\Delta x\,\Delta y\,\Delta z) \qquad (1)$$

where $\Delta x\Delta y\Delta z$ is the volume into which pollution is input at a rate of E over a time period t and C is the concentration of the pollution (i.e., mass per unit volume). The dimensions Δx and Δy could correspond to the horizontal dimensions of a valley, or to that portion of the valley over which the pollution spreads, while Δz would be the layer in the atmosphere into which the pollution is ejected. In a daytime, well-mixed boundary layer, this layer would correspond to the distance from the surface to the inversion height, whereas in a stable, stratified pool of cold air, this would correspond to some fraction of the inversion height. The time, t, would correspond to the length of time (i.e., persistence) of the trapped circulation, while E is the input of pollution above some baseline (which could be zero). C represents the maximum uniformly distributed concentration of an elemental chemical (e.g., sulfur, carbon) over the volume $\Delta x\Delta y\Delta z$ since deposition to the surface is ignored. While this conceptually simple model needs to be validated, it is a plausible approach to represent pollution build-up in trapping valleys.

In order to illustrate the use of Eq. (1) to assess air quality impacts for a valley which acts to some extent as a trapping valley, the possible effects of a source in the Grand Valley of Colorado near Grand Junction on Colorado National Monument will be assessed for a typical wintertime stagnation event. The variables in Eq. (1) are defined as

$$\begin{aligned} \Delta z &= \beta z_i = \beta(2\text{ km}) \quad \beta \le 1 \\ \Delta y &= 20\text{ km} \\ \Delta x &= \alpha\Delta y \qquad\qquad \alpha > 1 \qquad (2) \\ t &= 9\text{ days} \\ E &= 25\text{g s}^{-1}\text{ of S} \end{aligned}$$

where the sulfur is primarily in the form of SO_2.

In Eq. (2), β represents the fraction of the inversion height into which the pollution is input and diffused. The inversion height is estimated from the climatological analyses of Hanson and McKee (1983), and is below the elevation of the valley sides. The distance Δy is the approximate width of the valley, while α represents the distance of pollution dispersal along the valley with respect to the valley width. The time, t, of an episode is selected as nine days based on the information discussed in Section 2. E is a realistic estimate of SO_2 input from a relatively small industrial facility. Using these values, Eq. (1) can be rewritten as

Table 3. Selected solutions for (3) for various values of α and β.

C	$\beta = 1$	$\beta = 0.1$
$\alpha = 10$	2.43×10^{-6} g m^{-3}	2.43×10^{-5} g m^{-3}
$\alpha = 20$	1.21×10^{-6} g m^{-3}	1.21×10^{-5} g m^{-3}

$$C\left(\mathrm{g\,m^{-3}}\right) = \frac{(2.43 \times 10^{-5})}{\alpha\beta} \qquad (3)$$

The 24-h primary air quality standard for SO_2 at a Class I air quality area in the United States is expected to be the most sensitive to violation as a result of a nine-day stagnation event. The 24-h standard is 5×10^{-6} g m^{-3}. Thus Eq. (3) indicates a violation if the volume covered by $\Delta x\ \Delta y\ \Delta z$ includes a Class I area and $\alpha\beta < 5$.

Colorado National Monument has been categorized as a state of Colorado equivalent to a Federal Class I area for SO_2. The state nomenclature refers to it as a Category I area. Thus depending on the values of α and β, and the site of the emission with respect to the Monument, a violation could be shown to exist.

Table 3 illustrates values of C for different values of α and β. In a stable layer of pooled air, it is expected that β would be on the order of 10% of the inversion height since a surface non-buoyant emission would tend to be confined close to the ground while an elevated release would stabilize around the effective stack height (as long as the effective stack height remains below the inversion). The along valley direction for the example is more difficult to estimate, however, but a distance of 200 km ($\alpha = 10$) is likely to represent the largest horizontal area covered.

Local versus long-range transport

The discussion in the last section focused on a situation in which only local recirculation and accumulation of pollution is important. In the more general case, transport of pollution into a region is of concern.

Using the synoptic classification scheme presented in Section *Air quality climatology*, it is straightforward to argue that long-range transport becomes important when a significant synoptic flow exists. The synoptic flow in the lower troposphere can be estimated from the 850 mb and 700 mb winds, and from the surface pressure gradient. A unidirectional wind of 5 m s^{-1} at 850 mb, for example, would transport a plume of pollution 384 km after 24 h. A wind of 15 m s^{-1} would result in a movement of 1152 km.

While winds are seldom so uniform, using these relative estimates of the influence of wind speed on transport, it is obvious that pollution releases near regions of moderate or strong synoptic flow will be subject to long-range transport, while lighter synoptic flow will result in less movement and a greater importance of local circulations.

Near the centers of synoptic Categories 4 and 5 (the polar and subtropical highs) are regions with light synoptic flow, while a larger horizontal pressure gradient force, and thus stronger synoptic winds occur near extratropical cyclones. Current tools used to assess transport (e.g., the ARL-ATAD model; see Artz 1982), apply observational data to characterize transport. Unfortunately, due to insufficient measurement data density, these tools are only able to characterize the longer range transport, but not the movement of air associated with local circulations. Table 2 summarizes whether long- or local range transport is expected to dominate for each of the synoptic categories. Stocker et al. (1990) used observed transport patterns of balloons to demonstrate the differences of the ARL-ATAD model.

Use of a mesoscale model to characterize local circulations

Since the existing synoptic observation network is unable to characterize local circulations, such as occur in synoptic Categories 4 and 5, other techniques must be found. In lieu of an extensive measurement network in a local area, the only tools available are models. In this section, one such tool will be discussed.

Since the early 1970's, extensive research has been made into the study of thermally-forced mesoscale systems by our research group (Table 4). With respect to the impact of local circulations on air quality and local transport under synoptic Categories 4 and 5, this mesoscale meteorological model has been used

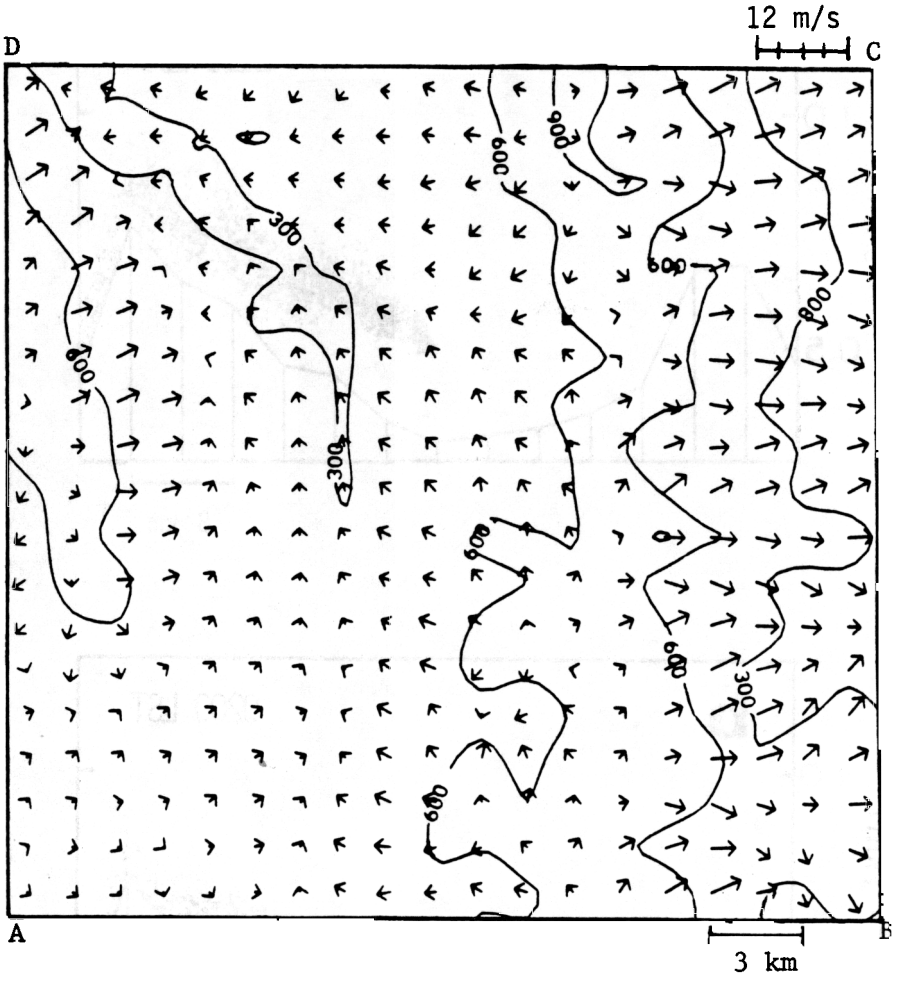

Fig. 8. Simulated horizontal wind velocities at 3.5 m height on 18 July 1977 at 0310 LST. Contours indicate elevation of terrain in meters. The top of the figure is towards the northeast (Pielke et al. 1985).

to simulate wind flow and turbulence characteristics in complex terrain. The output of this model is used to integrate a so-called Lagrangian Particle Dispersion (LPD) model in which releases of a number of particles from elevated or surface locations are used to simulate the dispersion of pollution from actual or planned sources. This dispersion is a result of both turbulent diffusion and differential vertical and horizontal advection. Our approach has been summarized in Pielke et al. (1983).

To illustrate this approach with respect to an existing federally legislated wilderness area, the meteorological model has been integrated in order to simulate the local flows that developed on 18 July 1977 in and near Shenandoah National Park, Virginia. About 79 000 acres of the park are legislated wilderness areas. Figure 8 illustrates the local wind flow at 3.5 m above ground level as predicted by the model. The output from the meteorological model is used to simulate a hypothetical release from an elevated source near Elkton, Virginia (Fig. 9). This location corresponds to the site of a brewery. Existing EPA-approved regulatory tools indicated that the Class I increment for SO_2 would not be violated at any point within the park as a result of this facility. The results in Fig. 9, however, raise serious questions as to the accuracy of the EPA-approved results since the recirculation (and resultant accumulation) of pollution associated with the mountain-valley flow illustrated in Fig. 8 were ignored in the regulatory models. Work is continuing under National Park sponsorship to quantify expected concentration impacts on the park wilderness areas as a result of mountain-valley circulations; it appears that to some extent at

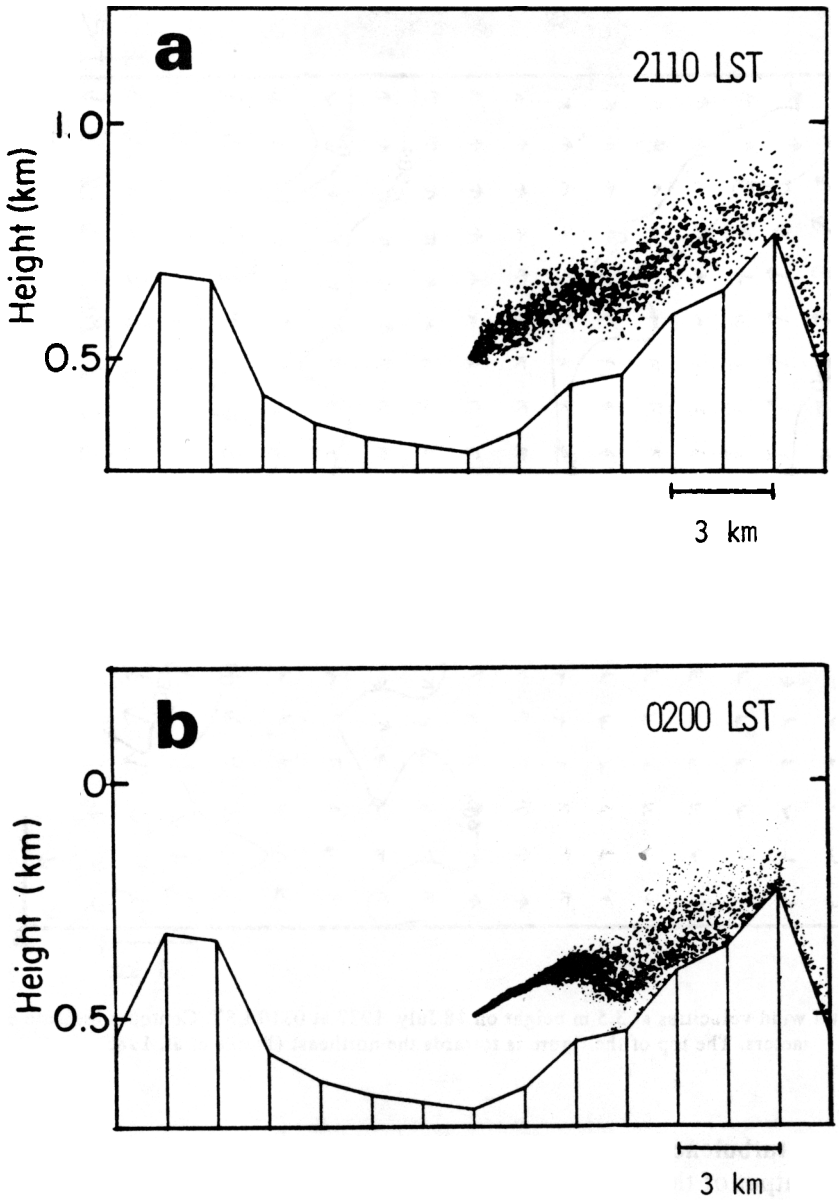

Fig. 9. Plot showing dispersion of particles continuously released at 60-second time intervals during a) two hours following sunset and b) the two-hour period following midnight. Release height is 200 m above ground level. The meteorological model applied to create Fig. 8 was used to generate these dispersion characteristics.

least, Shenandoah Valley can act as a trapping valley. Additional results, including effects on dry deposition, are discussed by Arritt (1988; 1990).

CONCLUSIONS

Using a straightforward synoptic climatological analysis scheme, it is shown that the potential for an area to experience air quality degradation due to local sources is highest under polar and subtropical highs. With respect to polar highs, the problem is most severe when the sun angle is low and snow covers the ground, and the polar high persists for a long period of time.

A simple algorithm is introduced which is designed to estimate worst-case impact in a trapping valley. The potential for the accumulation of air pollution in such valleys due to the persistence of a polar high in

a region, is ignored in current regulatory air quality assessments. Trapping valleys and synoptic flow stagnation often occur in wilderness areas.

Refined air quality assessments are shown to be possible using a mesoscale meteorological model and a pollution dispersion model. These tools permit quantitative assessments of pollution build-up from local sources as a result of the recirculation of the local air. This tool, along with the synoptic climatological classification scheme, also permits an evaluation of the fractional contribution of long range versus local sources since pollution releases near regions of moderate or strong synoptic flow will be subject to long-range transport while lighter synoptic flow will result in less movement and a greater importance of local circulations.

Acknowledgment — This work was sponsored by the National Park Service through Interagency Agreement #0475-4-8003 with the National Oceanic and Atmospheric Administration through agreement #CM0200 DOC-NOAA to the Cooperative Institute for Research in the Atmosphere (Project #5-31253). The authors gratefully appreciate that support. Dallas McDonald, Bryan Critchfield, and Tony Smith prepared the manuscript.

REFERENCES

Abbs, D.J. Observations and numerical modelling of southern Australian sea breezes. Ph.D. Dissertation, University of Melbourne, Meteorology Department. 1984:307pp.

Arritt, R.W. Numerical modeling of the effects of local source emissions on air quality in and around Shenandoah National Park. Report prepared for National Park Service, Dept. of Interior, Denver, CO 80225. 1988:136pp.

Arritt, R.W. Demonstration of a numerical modeling technique for estimating sulfur dioxide dry deposition due to local source emissions. J. Air Poll. Control Assoc. 1991. (In press)

Artz, Richard S. Comparison of methods of air parcel trajectory analysis for defining source-receptor relationships. M.S. Thesis, University of Virginia, Charlottesville. 1982:363pp.

Cotton, W.R.; Gannon, P.T.; Pielke, R.A. Numerical experiments on the influence of the mesoscale circulations on the cumulus scale. J. Atmos. Sci. 33:252-261;1976.

Dalu, G.A.; Cima, A. Three-dimensional air flow over Sardinia. Il Nuovo Cimento 6:453-472; 1983.

Diab, R.D.; Garstang, M. Assessment of wind power potential for two contrasting coastlines of South Africa using a numerical model. J. Climate Appl. Meteor. 23:1645-1659; 1984.

Everhart, W.C. The National Park Service, Boulder, CO, Westview Press; 1983: 197 pp.

Gannon, Patrick T. On the influences of surface thermal properties and clouds on the south Florida sea breeze. Ph.D. Dissertation, University of Miami, Coral Gables, Florida. 1976:152pp.

Garratt, J.R.; Physick, W.L. The inland boundary layer at low latitudes. II: Sea-breeze influences. Bound.-Layer Meteor. 33:209-231; 1985.

Hanson, K.R.; McKee, T.B. Potential for regional air pollution episodes in Colorado. Atmospheric Science Paper No. 375, Colorado State University, Department of Atmospheric Science, Fort Collins, CO; 1983.

Hjelmfelt, M.R. Numerical simulation of the effects of St. Louis boundary layer airflow and convection. Ph.D. Dissertation, University of Chicago, Chicago, IL; 1980.

Hjelmfelt, M.R. Numerical simulation of the effects on mesoscale boundary layer airflow and vertical air motion: Simulations of urban vs. non-urban effects. J. Appl. Meteor. 21:1239-1257; 1982.

Hjelmfelt, M.R.; W.A. Lyons; R.A. Pielke. Mesoscale spiral vortex embedded within a Lake Michigan snow squall band: Observations and model simulation. In: Proc. Ist Conference on Mesoscale Meteorology, Norman, Oklahoma, May 1983. Available from: American Metereological Society, Boston, MA.

Lindsey, C.G. Analysis of coastal wind energy regimes. M.S. Thesis, University of Virginia, Charlottesville. 1980:183 pp.

Lyons, W.A.; Schuh, J.A.; McCumber, M. Comparison of observed mesoscale lake breeze wind fields to computations using the University of Virginia Mesoscale Model. In: Proc. 4th Symposium on Turbulence, Diffusion, and Air Pollution, Reno, Nevada. 1979a:572-575. Available from: American Metereological Society, Boston, MA.

Lyons, W.A.; Schuh, J.A.; Keen, C.S.; McCumber, M.; McNider, R. Trajectory observations compared to computations using a regional mesoscale model to study air pollution in a lake breeze. In: Proc. 72nd annual meeting of the Air Pollution Control Association, Cincinnati, Ohio, 79-15.3; 1979b: 22 pp. Available from: Air Pollution Control Association, Pittsburgh, PA.

Lyons, W.A.; Calby, R.H.; Keen, C.S. The impact of mesoscale convective systems on regional visibility and oxidant distributions during persistent elevated pollution episodes. J. Climate Appl. Meteor. 25:1518-1531; 1986.

Mahrer, Y.; Pielke, R.A. The numerical simulation of the airflow over Barbados. Mon. Wea. Rev. 104:1392-1402; 1976.

McCumber, M.C. A numerical simulation of the influence of heat and moisture fluxes upon mesoscale circulation. Ph.D. Dissertation, Department of Environmental Sciences, University of Virginia, Charlottesville. 1980: 255 pp.

McKee, T.B.; O'Neal, R.D. The role of valley geometry and energy budget in the formation of nocturnal valley winds. J. Appl. Meteor. 28:445-456; 1988.

McNider, R.T. Investigation of the impact of topographic circulations on the transport and dispersion of air pollutants. Ph.D. Dissertation, Department of Environmental Sciences, University of Virginia, Charlottesville; 1981: 210 pp.

McNider, R.T.; Pielke, R.A. Diurnal boundary layer development over sloping terrain. J. Atmos. Sci., 3:2198-2212; 1981.

McNider, R.T.; Pielke, R.A. Numerical simulation of slope and mountain flows. J. Climate Appl. Meteor. 10:1441-1453; 1984.

McNider, R.T.; Anderson, K.J.; Pielke, R.A. Numerical simulation of plume impaction. In: Proc. 3rd Conference on Application of Air Pollution Meteorology, AMS, January, San Antonio, Texas, 126-129; 1982. Available from: AMS, Boston, MA.

Mizzi, A.P. A numerical investigation of the mesoscale atmospheric circulation in the Oregon coastal zone with a coupled atmosphere-ocean model. M.S. Thesis, University of Virginia, Charlottesville; 1981.

Mizzi, A.P.; Pielke, R.P. A numerical study of the mesoscale atmospheric circulation observed during a coastal upwelling event on August 23,1972. Part I: Sensitivity studies. Mon. Wea. Rev. 112:76-90; 1984.

Okeyo, A.E. A two-dimensional model of the lake-land and sea-land breezes over Kenya. M.S. thesis, Department of Meteorology, University of Nairobi, Nairobi, Kenya. 1982:244pp.

Pielke, R.A. A three-dimensional numerical model of the sea breezes over south Florida. Mon. Wea. Rev. 102:115-139; 1974.

Pielke, R.A. The role of mesoscale numerical models in very short-range forecasting. In: Browning, K. ed. Nowcasting, Academic Press, New York, N.Y.; 1982:207-221.

Pielke, R.A. Mesoscale meteorological modeling. Academic Press, New York, NY. 1984:612pp.

Pielke, R.A.; Mahrer, Y. The numerical study of the air flow over mountains using the University of Virginia mesoscale model. J. Atmos. Sci. 32:2144-2155; 1975.

Pielke, R.A.; Mahrer, Y. Verification analysis of the University of Virginia three-dimensional mesoscale model prediction over south Florida for July 1, 1973. Mon. Wea. Rev. 106:1568-1589; 1978.

Pielke, R.A.; Mcnider; R.T. Segal, M.; Mahrer, Y. The use of a mesoscale numerical model for evaluations of pollutant transport and diffusion in coastal regions and over irregular terrain. Bull. Amer. Meteor. Soc. 64:243-249; 1983.

Pielke, R.A.; Yu, C-H.; Arritt, R.W.; Segal, M. Mesoscale air quality under stagnant conditions. In: Proc. Air Pollution Effects on Parks and Wilderness Areas Conference, May 1984, Mesa Verde National Park, CO; 1985:71-103. Available from: Institute for Urban and Public Policy Research, University of Colorado at Denver, CO.

Pielke, R.A.; Garstang, M.; Lindsey, C.; Gusdorf, J. Use of a synoptic classification scheme to define seasons. Theor. Appl. Clim. 38:57-68;1987.

Segal, M.; Pielke, R.A. Numerical model simulation of human biometeorological heat load conditions—summer day case study for the Chesapeake Bay area. J. Appl. Meteor. 20:735-349; 1981.

Segal, M.; Mcnider, R.T.; Pielke, R.A.; Mcdougal, D.S. A numerical model simulation of the regional air pollution meteorology of the greater chesapeake bay area—summer day case study. Atmos. Environ. 16:1381-1397; 1982a.

Segal, M.; Mahrer, Y.; Pielke, R.A. Numerical study of wind energy characteristics over heterogenous terrain—Central Israel case study. Bound.-Layer Meteor. 22:373-392; 1982b.

Segal, M.; Mahrer, Y.; Pielke, R.A. Application of a numerical mesoscale model for the evaluation of seasonal persistent regional climatological patterns. J. Appl. Meteor. 21:1754-1762; 1982c.

Segal, M.; Mahrer, Y.; Pielke, R.A. A study of meteorological patterns associated with a lake confined by mountains—the Dead Sea case. Quart. J. Roy. Meteor. Soc. 109:549-564; 1983a.

Segal, M.; Pielke, R.A.; Mahrer, Y. On climatic changes due to a deliberate flooding of the Qattara depression (Egypt). Climatic Change 5:73-83; 1983b.

Segal, M.; Mahrer, Y.; Pielke, R.A. On some meteorological patterns at the Dead-Sea area during advective Sharav situations. Israel J. Earth Sci. 33:76-83; 1983c.

Snow, J.W. Coastal zone wind power assessment. Ph.D. Dissertation, University of Virginia, Charlottesville. 1981:244pp.

Stocker, R.A.; Pielke, R.A.; Verdon, A.J.; Snow, J.T. Characteristics of plume releases as depicted by balloon launchings and model simulations. J. Appl. Meteor. 29:53-62; 1990.

Trewartha, G.T.; Horn, L.H. An introduction to climate. New York: McGraw-Hill Book Company. 1980:416 pp.